nature neuroscience

ARTICLES

Mammalian *Gcm* genes induce *Hes5* expression by active DNA demethylation and induce neural stem cells

Seiji Hitoshi[1,2], Yugo Ishino[1,2], Akhilesh Kumar[1,2], Salma Jasmine[1,2], Kenji F Tanaka[1,2], Takeshi Kondo[3], Shigeaki Kato[3], Toshihiko Hosoya[4], Yoshiki Hotta[5] & Kazuhiro Ikenaka[1,2]

Signaling mediated by Notch receptors is crucial for the development of many organs and the maintenance of various stem cell populations. The activation of Notch signaling is first detectable by the expression of an effector gene, *Hes5*, in the neuroepithelium of mouse embryos at embryonic day (E) 8.0–8.5, and this activation is indispensable for the generation of neural stem cells. However, the molecular mechanism by which *Hes5* expression is initiated in stem-producing cells remains unknown. We found that mammalian Gcm1 and Gcm2 (glial cells missing 1 and 2) are involved in the epigenetic regulation of *Hes5* transcription by DNA demethylation independently of DNA replication. Loss of both *Gcm* genes and subsequent lack of *Hes5* upregulation in the neuroepithelium of E7.5–8.5 *Gcm1*$^{-/-}$; *Gcm2*$^{-/-}$ mice resulted in the impaired induction of neural stem cells. Our data suggest that *Hes5* expression is serially activated first by Gcms and later by the canonical Notch pathway.

Neural stem cells, which respond to basic fibroblast growth factor (FGF2) and proliferate in culture to form neurospheres, emerge in the nervous tissue of mouse embryos at E8.5 (refs. 1,2). Activation of Notch signaling is indispensable for the generation and maintenance of FGF2-responsive neural stem cells[3–5], and upregulation of *Hes5* expression occurs in the mouse forebrain at the same stage[2]. Despite the fact that *Hes5* is one of the target genes of Notch signaling[6], its expression remains detectable in null mutants of Notch pathway genes[7,8]. Although *Hes5* mRNA is absent in entire *Rbpj*$^{-/-}$ embryos at E8.5, which present the severest phenotypes among null mutants of Notch pathway genes, *Hes5* is expressed in the midbrain and hindbrain of E8.5 *Notch1*$^{-/-}$ embryos[7]. Furthermore, although *Hes5* expression is abolished in the neural tube in embryos deficient for both presenilin 1 and 2 (*Psen1* and *Psen2*) genes, which lack components of γ-secretase indispensable to activate canonical Notch signaling, low levels of *Hes5* expression remain in the midbrain and hindbrain[8]. These observations suggest that a signal pathway other than canonical Notch signaling upregulates *Hes5* expression in the nervous tissue of early embryos.

The *gcm* gene was first identified in *Drosophila* through the examination of a loss-of-function mutant, in which presumptive glial cells that arise from neural precursors in the CNS and PNS differentiate into neurons instead of glia[9,10]. Conversely, ectopic expression of *gcm* in neural lineage cells resulted in the transformation of presumptive neurons into glia[9,10]. Thus, *gcm* in *Drosophila* acts as a binary switch gene that determines whether neural precursors become neurons or glia[11]. *Drosophila gcm* and its homolog *gcm2* encode transcription factors with a unique DNA-binding domain, called the GCM domain, and regulate a number of glial-related and other genes[12–14]. In contrast to the strong phenotypes of *gcm* loss-of-function and gain-of-function mutants in *Drosophila*, the roles of the mammalian orthologs *Gcm1* and *Gcm2* in the nervous system remain elusive[15,16].

Here we show that mammalian Gcm proteins are crucial for the demethylation of methylated CpGs in the promoter region of *Hes5* and that this demethylation by Gcms is an active process that does not require DNA replication. On the basis of our findings, we propose that, unlike *Drosophila gcm*, which acts as a binary switch, mammalian Gcms function as a selective signal to direct neuroepithelial cells of early embryos to acquire stem cell properties.

RESULTS

Hes5 expression is suppressed by DNA methylation

To elucidate the regulatory mechanisms that contribute to the induction of *Hes5* expression in mouse embryos during E7.5–9.5, we used bisulfite sequencing to analyze DNA methylation status in the *Hes5* promoter, which contains two RBP-J binding sites. We found that eight CpG sites around the second RBP-J binding site were variously methylated and that those eight sites were highly methylated in E7.5 embryos but completely demethylated by E9.5 (**Fig. 1a**), which is consistent with the expression of *Hes5* in the head primordium at E8.5 and afterwards, but not before E7.5 (ref. 2).

We also found that the methylation frequency of those eight CpG sites around the second RBP-J binding site was lower in Neuro2a mouse neuroblastoma cells than that in non-neural STO fibroblasts (**Fig. 1b**). Chromatin immunoprecipitation (ChIP) analysis showed that methylation of CpG sites in the proximal promoter region of *Hes5* gene abolished the binding of RBP-J to the *Hes5* promoter (**Fig. 1c**,**d**), which is essential for the transduction of canonical Notch signaling to upregulate *Hes5* expression[6]. Accordingly, Notch1 intracellular

[1]Division of Neurobiology and Bioinformatics, National Institute for Physiological Sciences, Okazaki, Japan. [2]Department of Physiological Sciences, School of Life Sciences, Graduate University for Advanced Studies, Okazaki, Japan. [3]Institute of Molecular and Cellular Biosciences, University of Tokyo, Tokyo, Japan. [4]Hosoya Research Unit, Brain Science Institute, RIKEN, Wako, Saitama, Japan. [5]Research Organization of Information and Systems, Tokyo, Japan. Correspondence should be addressed to S.H. (shitoshi-tky@umin.ac.jp).

Received 20 January; accepted 13 June; Published online 17 July 2011; doi:10.1038/nn.2875

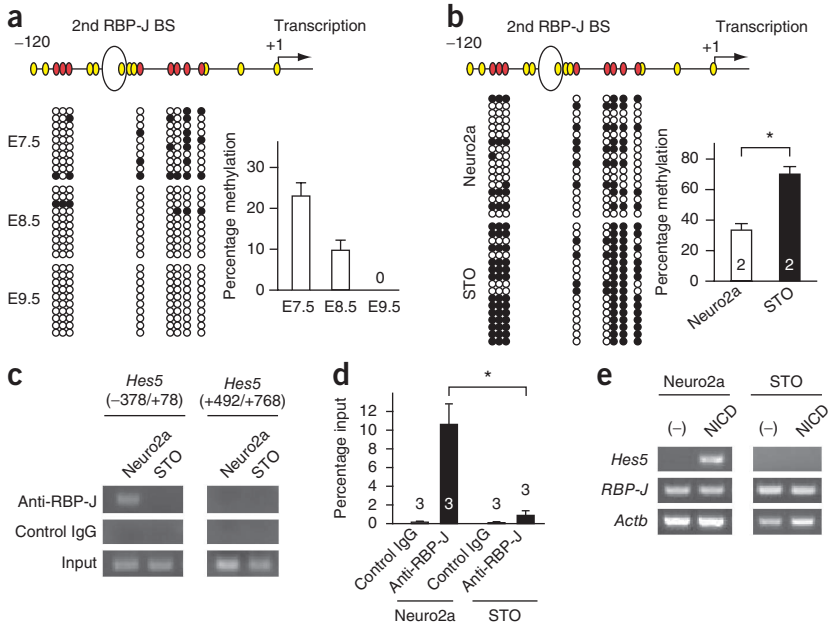

Figure 1 DNA methylation in the *Hes5* promoter. (**a**,**b**) Top, promoter region (bases −120 to +1) of *Hes5* containing the second RBP-J binding site (BS; large white oval) and CpG sites (small ovals). Eight CpG sites that are variously methylated are shown in red and other nonmethylated sites in yellow. Bottom left, methylation status of the *Hes5* promoter analyzed by bisulfite sequencing. Closed and open circles indicate methylated and non-methylated CpG sites, respectively. Bottom right, methylation frequency of the CpG sites in the *Hes5* proximal promoter region. (**a**) Developmental course of methylation status of the *Hes5* promoter region in the head primordium. Tissues from several embryos were pooled and two or more independent experiments were carried out. (**b**) Methylation status of the *Hes5* promoter in Neuro2a and STO cells. (**c**,**d**) ChIP analysis of Neuro2a and STO cells using an antibody to RBP-J, followed by PCR for the promoter region containing RBP-J binding sites (−378 to +78) or downstream region (+492 to +768) (**c**) and qPCR analysis (**d**). (**e**) RT-PCR for *Hes5* and *Rbpj* expression in Neuro2a and STO cells after transfection of NICD cDNA. Error bars indicate s.e.m. and *n* values are shown in or above columns. $*P < 0.05$ by Student's *t* test.

domain (NICD), an active form of Notch1 receptor, induced *Hes5* expression in Neuro2a cells but not in STO cells (**Fig. 1e**).

Gcm1 and 2 demethylate the *Hes5* promoter

To identify factors that interact with the *Hes5* promoter, we scrutinized the promoter region of the *Hes5* gene and found GCM binding sites[13,14,17] (**Supplementary Fig. 1**). We detected *Gcm1* mRNA in mouse embryos as early as E6.5 and observed transient *Gcm2* mRNA expression around E7.5, which is just before the induction of *Hes5* expression (**Fig. 2a**). Consistent with the fact that Gcms act as transcriptional activators[11], overexpression of mouse *Gcm1* or *Gcm2* upregulated *Hes5* expression in Neuro2a cells (**Supplementary Fig. 1a**). The transactivating activity of Gcms depended on RBP-J because it was no longer seen when we also tranfected the cells with a dominant-negative form of RBP-J (**Supplementary Fig. 1b**). Luciferase reporter assays using the *Hes5* promoter were consistent with these conclusions and further showed that the second of four putative GCM-binding sites

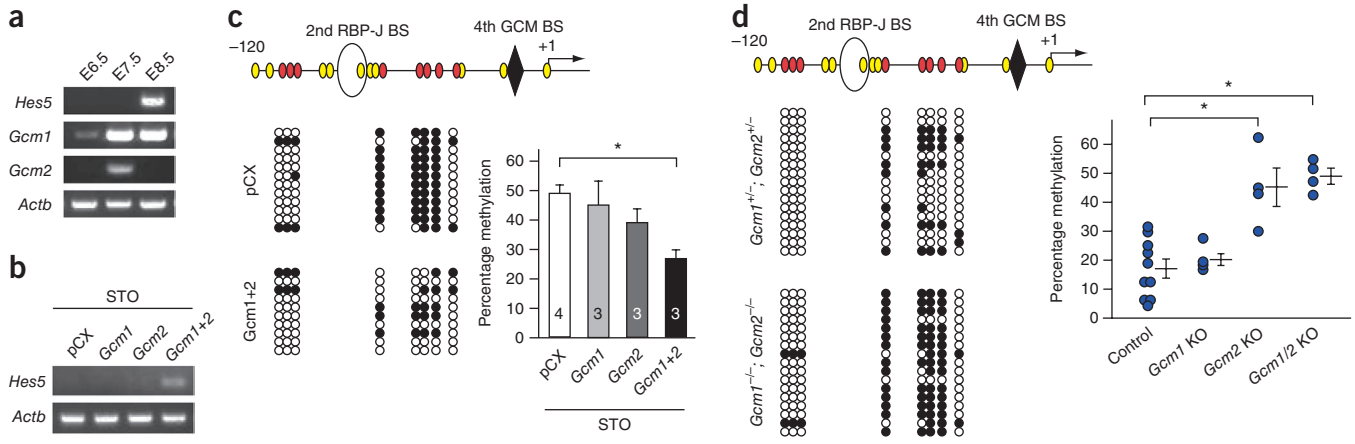

Figure 2 Gcms are responsible for the demethylation of the *Hes5* promoter. (**a**) RT-PCR for *Hes5*, *Gcm1* and *Gcm2* expression in the E6.5 whole embryo, E7.5 head primordium and E8.5 forebrain. (**b**) RT-PCR for *Hes5* expression in STO cells after transfection of *Gcm1*, *Gcm2* or both. (**c**,**d**) Methylation status analyzed by bisulfite sequencing using genomic DNA extracted from STO cells transfected with pCX expression vector, or vectors encoding *Gcm1* or *Gcm2* or both (**c**), or using genomic DNA from the forebrain and midbrain of E8.33 *Gcm1* and *Gcm2* mutants (**d**). Top, promoter region (bases −120 to +1) of *Hes5* containing the second RBP-J binding site (BS; large white oval), fourth GCM binding site (black diamond) and CpG sites (small ovals). Eight CpG sites that are variously methylated are shown in red and other nonmethylated sites in yellow. Bottom left, methylation status of the *Hes5* promoter analyzed by bisulfite sequencing. Closed and open circles indicate methylated and nonmethylated CpG sites, respectively. Right, methylation frequency of the CpG sites in the *Hes5* proximal promoter region. Control: $Gcm1^{+/+}; Gcm2^{+/+}$, $Gcm1^{+/-}; Gcm2^{+/+}$, $Gcm1^{+/+}; Gcm2^{+/-}$ and $Gcm1^{+/-}; Gcm2^{+/-}$. *Gcm1* KO: $Gcm1^{-/-}; Gcm2^{+/+}$ and $Gcm1^{-/-}; Gcm2^{+/-}$. *Gcm2* KO: $Gcm1^{+/+}; Gcm2^{-/-}$ and $Gcm1^{+/-}; Gcm2^{-/-}$. *Gcm1/2* KO: $Gcm1^{-/-}; Gcm2^{-/-}$. Error bars, s.e.m.; *n* values are shown in columns. $*P < 0.05$ by one-way ANOVA followed by Dunnett's *post hoc* comparison (**c**) or by Kruskal-Wallis test followed by Dunn's multiple comparison test (**d**).

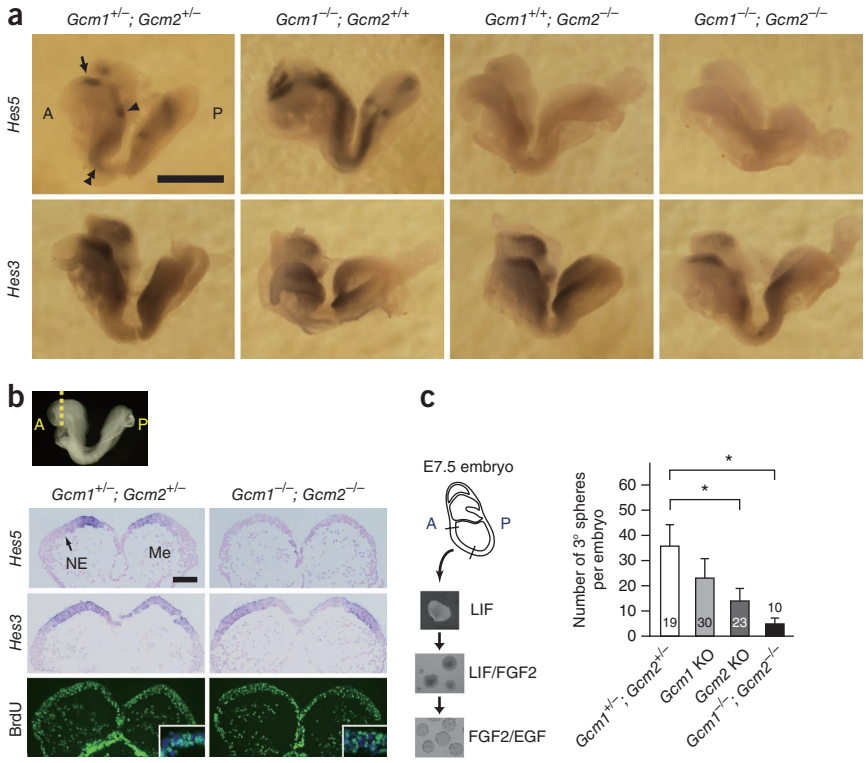

Figure 3 Gcms are indispensable for *Hes5* induction and neural stem cell generation. (**a**) Analysis of *Hes5* (top) and *Hes3* (bottom) expression in E8.33 mutant embryos by whole mount *in situ* hybridization. *Hes5* mRNA is present in the portion of midbrain (arrow) and hindbrain (arrowhead) and neural tube (double arrowhead) in E8.33 control embryos. The reduction of *Hes5* expression in $Gcm2^{-/-}$ mutants varied embryo to embryo, and the severest one is shown. $n \geq 3$ for *Hes5* and $n \geq 2$ for *Hes3*. (**b**) Top, dotted line in E8.33 embryo indicates the level of coronal sections. Bottom, *in situ* hybridization for *Hes5* and *Hes3* and immunohistochemistry for BrdU. Insets, higher magnification pictures for BrdU and Hoechst. NE, neuroectoderm; Me, mesenchymal cells. (**c**) Left, scheme of *in vitro* induction of neural stem cells from E7.5 embryos. Right, bar graphs of the number of tertiary (3°) FGF2/EGF-responsive spheres from E7.5 *Gcm1* and *Gcm2* mutants. Scale bars: 0.5 mm (**a**), 100 µm (**b**). Error bars represent s.e.m. and *n* values are shown in or above columns. $^*P < 0.05$ by Kruskal-Wallis test followed by Dunn's multiple comparison test.

contributed more to Gcm1- and Gcm2-mediated expression than the other three sites; there was no reporter expression when this binding site was deleted or mutated (**Supplementary Fig. 1c**). We used ChIP to verify that Gcm1 interacted directly with the GCM binding sites in the *Hes5* promoter region (**Supplementary Fig. 2**). In samples prepared from E8.5 mouse embryos, immunoprecipitation with antibodies to GCM1 yielded an enrichment of chromatin containing the second GCM binding site (**Supplementary Fig. 2a**,**b**) and this enrichment was abolished in the absence of *Gcm1* (**Supplementary Fig. 2c**,**d**).

Unlike Neuro2a cells, STO cells were resistant to the induction of *Hes5* by overexpression of either *Gcm1* or *Gcm2* (**Fig. 2b**). However, overexpression of both *Gcm1* and *Gcm2* induced STO cells to express *Hes5* (**Fig. 2b**). STO cells overexpressing both *Gcm1* and *Gcm2* had significantly lower CpG methylation in the *Hes5* promoter than control cells ($F_{(3,9)} = 4.732$, $P = 0.0301$; **Fig. 2c**). The lack of *Hes5* induction by either Gcm1 or Gcm2 can be explained by observations that DNA methylation around the second RBP-J binding site prevents RBP-J from binding to the *Hes5* promoter (**Fig. 1c**,**d**) and that the enhancement of promoter activity by Gcms was no longer detected when the RBP-J binding sites were deleted from the *Hes5* promoter or when the dominant-negative RBP-J was also transfected (**Supplementary Fig. 1b**,**c**).

To investigate whether *Gcm1* and *Gcm2* were involved in the demethylation of the *Hes5* promoter in E7.5–E9.5 mouse embryos, we generated mice mutant for *Gcm1* and *Gcm2* (**Supplementary Fig. 3**). As reported earlier, *Gcm1* homozygous mutants died around E9.5–10.5 owing to placental dysfunction[18]. $Gcm1^{-/-}$; $Gcm2^{-/-}$ double-knockout embryos appeared to develop normally until E8.5, but were lost before the turning (axial rotation of the embryo; **Supplementary Table 1**). Using $Gcm1^{-/-}$; $Gcm2^{-/-}$ mutants at E8.33, we examined the methylation status of the *Hes5* promoter in the forebrain and midbrain, and found that demethylation was impaired in both *Gcm2* knockout and *Gcm1/2* double knockout mutants ($P = 0.002$; **Fig. 2d**). These data suggest that Gcm2 that is transiently expressed in mouse embryos at E7.5 is important, with Gcm1, for the demethylation of the *Hes5* promoter in early embryos.

Loss of *Hes5* upregulation in *Gcm* mutants

Reduced demethylation of the *Hes5* promoter in *Gcm1* and *Gcm2* mutants prompted us to examine *Hes5* expression in mutant embryos at E8.33. In E7.5–9.5 wild-type embryos, *Hes3* and *Hes5* showed compensatory expression, with *Hes3* shrinking and *Hes5* expanding[19]. Although $Gcm1^{+/-}$; $Gcm2^{+/-}$ and $Gcm1^{-/-}$ mutants showed similar *Hes5* expression to that of wild-type embryos, *Hes5* expression was reduced in *Gcm2* null mice, and was abolished in $Gcm1^{-/-}$; $Gcm2^{-/-}$ double-null mutants (**Fig. 3a**,**b**). This reduction in *Hes5* was probably not due to the growth retardation or death of the mutants, as the numbers of somite pairs (usually 5–8) were comparable among wild-type and mutant littermates, and neither cell proliferation nor *Hes3* expression were affected in mutant brains (**Fig. 3a**,**b**). Thus, in $Gcm1^{-/-}$; $Gcm2^{-/-}$ embryos, the induction of *Hes5* expression was specifically impaired.

We investigated whether neural stem cells that responded to FGF2 and epidermal growth factor (EGF) could be generated in the absence of both *Gcm* genes. Because of the early lethality of $Gcm1^{-/-}$; $Gcm2^{-/-}$ embryos, we used an *in vitro* culture of E7.5 epiblasts[2] (**Fig. 3c**). Whereas the formation of secondary leukemia inhibitory factor (LIF)/FGF2-responsive spheres was preserved among mutants, the lack of either *Gcm1* or *Gcm2* reduced the efficiency of the derivation of tertiary neurospheres (**Supplementary Fig. 4**). The mean number of tertiary FGF2/EGF-responsive neurospheres was reduced to 38% in cultures from *Gcm2* knockout embryos and to 13% in cultures from *Gcm1/2* double knockout embryos as compared to those from $Gcm1^{+/-}$; $Gcm2^{+/-}$ embryos ($P = 0.0054$; **Fig. 3c**). Owing to the scarcity of $Gcm1^{-/-}$; $Gcm2^{-/-}$ embryos, we used cells derived from E7.5 *Gcm2* knockout embryos for a rescue experiment. Transduction of *Hes5* by a retrovirus restored the generation of tertiary FGF2/EGF-responsive neurospheres (8.571 ± 3.872 (mean ± s.e.m.) for control retrovirus ($n = 7$), 35.43 ± 7.767 for *Hes5* retrovirus ($n = 7$); $P = 0.0124$ by Mann Whitney test), suggesting that the expression of *Hes5* induced by Gcm1 and Gcm2 in E7.5–8.5 embryos is required for the generation of neural stem cells.

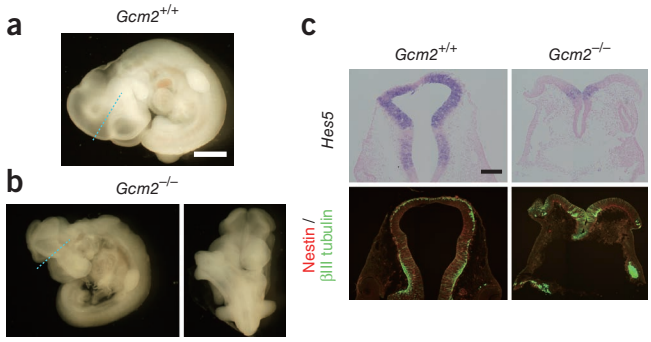

Figure 4 Abnormal neural development in *Gcm2* null mutants. (**a**,**b**) Gross morphology of E10.5 *Gcm2* mutant embryos. The lateral (**b**, left) and frontal (**b**, right) views of $Gcm2^{-/-}$ mutants show the opening of the anterior neuropore. (**c**) Coronal sections of the forebrain through the eye primordium (dotted line in **a** and **b**) analyzed by *in situ* hybridization for *Hes5* (top) or by immunostaining for nestin and βIII tubulin (bottom). Scale bars: 1.0 mm (**a**,**b**), 200 μm (**c**).

As a result of the reduction in *Hes5* expression in the brain at E8.33, abnormal neural development became apparent in some of *Gcm2* null embryos at E10.5 (**Fig. 4a–c**). A few $Gcm2^{-/-}$ embryos (2 out of 12 live embryos) appeared normal, which is consistent with the findings that the methylation status of the *Hes5* promoter in some of $Gcm2^{-/-}$ embryos was comparable to that of control littermates (**Fig. 2d**) and that the reduction in *Hes5* expression in E8.33 $Gcm2^{-/-}$ embryos was diverse. The discrepancy between our results and previous findings that *Gcm2* mutants develop normally except for aplasia of parathyroid glands and present few phenotypes in the CNS until adulthood[16] are due to the different genetic background, as we also observed few phenotypes in the brains of $Gcm2^{-/-}$ mice on the 129/Sv background. Ten out of twelve $Gcm2^{-/-}$ embryos at E10.5 had smaller brains than $Gcm2^{+/+}$ littermates and opening of the anterior neuropore (**Fig. 4b**). The abnormally extended neuroepithelium of E10.5 $Gcm2^{-/-}$ mutants showed less *Hes5* expression and premature and aberrant neuronal differentiation (**Fig. 4c**) as compared to littermate $Gcm2^{+/+}$ embryos.

Gcms suppress the radial migration of neural precursors

To determine whether Gcm1 and Gcm2 induce *Hes5* expression *in vivo*, we performed *in utero* electroporation of *Gcm* genes, along with a GFP marker, into the cortices of E14.5 mouse embryos. Overexpression of both *Gcm1* and *Gcm2* induced neural precursor cells to ectopically express *Hes5* in the intermediate zone (IMZ), in addition to the endogenous expression of *Hes5* in the ventricular zone and sub-ventricular zones (VZ/SVZ; **Fig. 5a**). Upregulation of *Hes5* should prevent neural precursors from differenting and from migrating radially. Consistent with this notion, overexpression of *Gcm1* and *Gcm2* reduced the migration of GFP^+ cells from VZ/SVZ to the cortical plate ($t_{(9)} = 2.838$, $P = 0.0195$ for VZ/SVZ; $t_{(9)} = 2.348$, $P = 0.0435$ for IMZ; $t_{(9)} = 3.032$, $P = 0.0142$ for cortical plate; **Fig. 5b**). We observed more $Pax6^+$ cells in the ventricular zone (51.36 ± 5.94 (mean ± s.e.m.) for control ($n = 4$), 69.86 ± 3.81 for *Gcm1* and *Gcm2* ($n = 7$), $t_{(9)} = 2.756$, $P = 0.0223$) and fewer $Tbr2^+$ cells in the SVZ (25.39 ± 0.77 for control ($n = 4$), 14.70 ± 1.76 for *Gcm1* and *Gcm2* ($n = 7$), $t_{(9)} = 4.377$, $P = 0.0018$; **Fig. 5c**). Defective neural precursor cell migration was more apparent 72 h after the electroporation

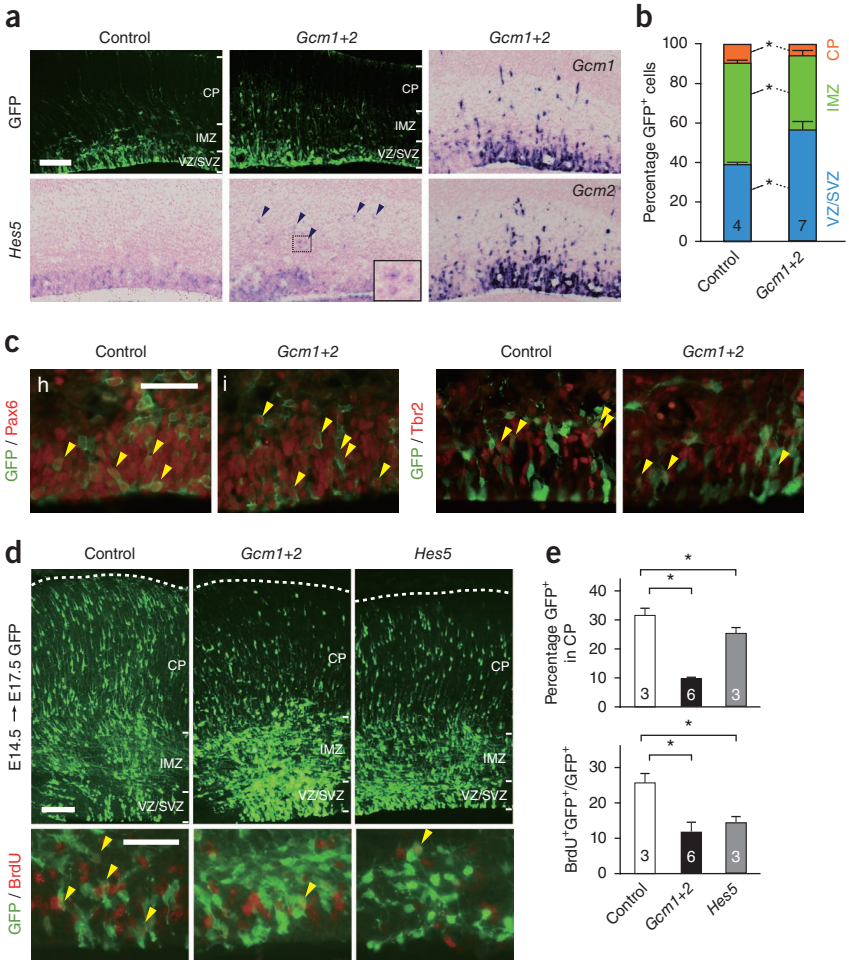

Figure 5 Gcms induce *Hes5* expression in embryonic brains. (**a**–**c**) *In utero* electroporation of pCX (control) or vectors encoding *Gcm1* and *Gcm2*, together with GFP expression plasmid, into the E14.5 mouse cortex and analysis after 24 h. (**a**) Embryos were either immunostained for GFP or *in situ* hybridized with probes for *Hes5*, *Gcm1* or *Gcm2*. Arrowheads, $Hes5^+$ cells; boxed area is magnified in inset. (**b**) Distribution of GFP^+ cells in VZ/SVZ, IMZ or cortical plate. (**c**) Double immunostaining for GFP and Pax6 (left) or GFP and Tbr2 (right). Arrowheads, double-positive cells. (**d**) *In utero* electroporation of pCX (control) or vectors encoding *Gcm1* and *Gcm2*, or *Hes5*, together with pCX-NLS-Cre expression plasmid into the E14.5 Z/EG reporter mouse cortex and analysis after 72 h. Embryos were immunostained for GFP (top) or GFP and BrdU (bottom). Arrowheads, double-positive cells. (**e**) Bar graphs showing the percentage of GFP^+ cells in the cortical plate (top) or $BrdU^+$ GFP^+ cells relative to total GFP^+ cells (bottom). Scale bars: 100 μm (**a**,**d**, top), 50 μm (**c**,**d**, bottom). Error bars, s.e.m.; *n* values shown in columns. $^*P < 0.05$ by Student's *t* test (**b**) or by one-way ANOVA followed by Dunnett's *post hoc* comparison (**e**).

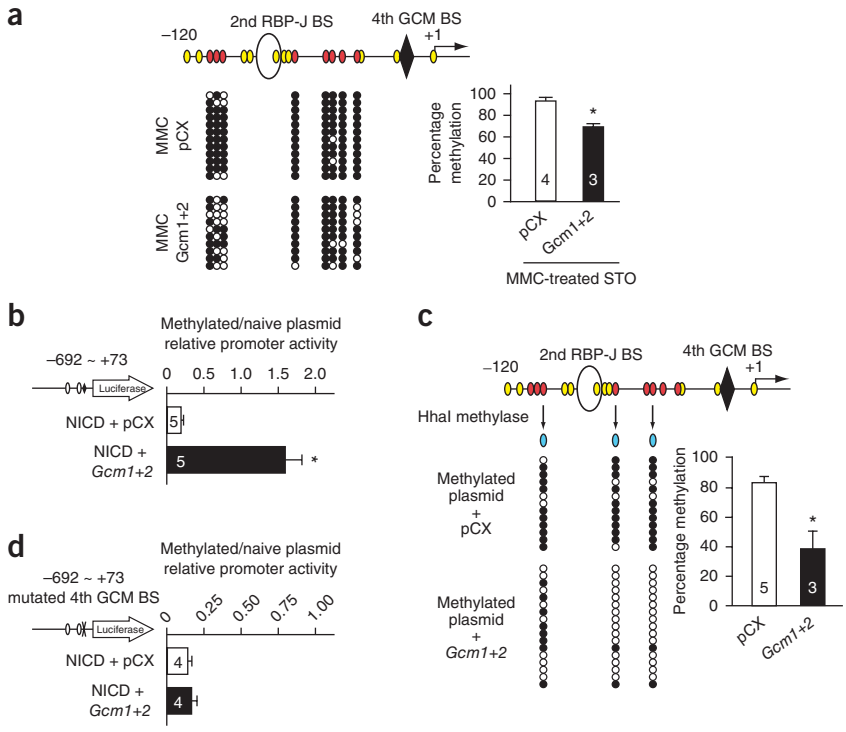

Figure 6 Gcms demethylate mitotically inactive DNA and methylated plasmids. (**a**) Methylation status of the *Hes5* promoter in mitomycin C (MMC)-treated STO cells transfected with pCX or vectors encoding *Gcm1* and *Gcm2*, together with GFP expression plasmid. After 72 h, transfected cells were collected by FACS against GFP and analyzed. Left, methylation status of the *Hes5* promoter analyzed by bisulfite sequencing. Closed and open circles indicate methylated and non-methylated CpG sites, respectively. Right, methylation frequency of the CpG sites in the *Hes5* proximal promoter region. (**b**,**d**) Ratio of relative promoter activities from methylated to those from naive luciferase reporter plasmids by NICD in the presence of either pCX alone, or both Gcm1-pCX and Gcm2-pCX plasmids. The reporter plasmids that contain intact *Hes5* promoter (**b**) or the promoter with mutations at the fourth GCM binding site (**d**) were transected into Neuro2a cells. (**c**) Methylation status of the HhaI-methylated reporter plasmid. Among eight CpG sites that are variously methylated (red ovals) in the promoter region (bases –120 to +1) of *Hes5* gene, three (blue ovals shown below) are methylated by HhaI. Bottom left, methylation status of the three HhaI-methylated CpGs in COS1 cells transfected with either pCX alone or both Gcm1-pCX and Gcm2-pCX. Closed and open circles indicate methylated and nonmethylated CpG sites, respectively. Right, methylation frequency of the HhaI-methylated CpG sites. Error bars, s.e.m.; *n* values shown in columns. $*P < 0.05$ by Student's *t* test.

of *Gcm1* and *Gcm2* and this phenotype was also apparent by the overexpression of *Hes5* (**Fig. 5d**). The percentage of GFP$^+$ cells in the cortical plate was lower in the brains overexpressing *Gcm1* and *Gcm2* or *Hes5* than in control brains ($F_{(2,9)} = 80.56$, $P < 0.0001$; **Fig. 5e**). There was a less severe migration defect in neural precursors overexpressing either *Gcm1* or *Gcm2* alone than in those overexpressing *Gcm1* and *Gcm2* in combination and ectopic expression of *Hes5* outside VZ/SVZ was only evident after the electroporation of *Gcm1* and *Gcm2* together (**Supplementary Fig. 5**), suggesting that the effects of *Gcm* genes are cumulative.

We assessed the proliferation of neural precursor cells by the incorporation of BrdU (**Fig. 5d**). The percentage of cells that was positive for both GFP and BrdU relative to total GFP$^+$ cells was lower in the brains that had received both *Gcm* genes or *Hes5* expression plasmids than in control brains ($F_{(2,13)} = 13.30$, $P = 0.0007$; **Fig. 5e**). These results suggest that overexpression of *Gcm* genes suppressed the proliferation of neural precursors at least in part through the action of *Hes5*, which is consistent with the finding that self-renewing neural stem cells elongate their cell cycle times during development[20].

Demethylation by Gcms is DNA replication independent

Methylation of CpG sites can be removed by two modes of demethylation; DNA replication-dependent passive and replication-independent active demethylation[21–23]. When the function of the maintenance DNA methyltransferase Dnmt1, which methylates cytosine in a newly synthesized DNA strand during cell division, is impaired, methylation of CpGs is passively lost. On the other hand, the molecular mechanism of active demethylation is poorly understood. We first investigated whether demethylation in the *Hes5* promoter by Gcms required chromosomal duplication, using mitotically inactivated STO cells treated with mitomycin C. Mitomycin C–treated STO cells overexpressing both *Gcm1* and *Gcm2* had significantly less CpG methylation in the *Hes5* promoter than those expressing vector alone ($t_{(5)} = 4.904$, $P = 0.0045$; **Fig. 6a**). This demethylation did not result from the induction of Hes5 by the overexpression of *Gcm* genes (**Fig. 2b**) because there was no significant demethylation in mitomycin C–treated STO cells overexpressing *Hes5* (**Supplementary Fig. 6a**). We then used a firefly luciferase reporter plasmid because the plasmid lacks a eukaryotic or mammalian viral origin of replication and is not duplicated in transfected cells[24]. The reporter plasmid containing the *Hes5* promoter region (bases –692 to +73), which did not mediate transcriptional activity by Gcm1 or Gcm2 (**Supplementary Fig. 1c**), was methylated *in vitro* by HhaI methylase. Whereas the naive reporter plasmid produced luciferase in the presence of NICD (51.44 ± 5.46-fold change (mean ± s.d.), $n = 3$), methylation of this plasmid abolished reporter gene expression (**Fig. 6b**), possibly owing to the binding of repressive molecule(s) that recognize methylated CpG[23]. However, when *Gcm1* and *Gcm2* were co-transfected with NICD, the promoter activity of NICD was restored ($t_{(8)} = 4.194$, $P = 0.003$; **Fig. 6b**). We also observed suppression of promoter activity by NICD using the methylated reporter plasmid and restoration of the suppressed promoter activity after expression of *Gcm1* and *Gcm2* in mitomycin C–treated Neuro2a cells ($t_{(3)} = 4.567$, $P = 0.0197$) and STO cells ($t_{(4)} = 3.015$, $P = 0.0394$; **Supplementary Fig. 6b**,**c**).

These results suggest that Gcm1 and Gcm2 triggered the demethylation of the plasmid. We verified this by recovering the plasmid from the transfected cells and analyzing its methylation status by bisulfite sequencing. Methylated CpG sites around the second RBP-J binding site, which had been methylated by HhaI, were demethylated in cells transfected with both *Gcm1* and *Gcm2* ($t_{(6)} = 4.329$, $P = 0.0049$; **Fig. 6c**). Gcms accessed the promoter region by binding to the fourth GCM binding site; when this binding site was mutated, NICD no longer restored promoter activity even in the presence of both Gcm1 and Gcm2 (**Fig. 6d**). Supporting this notion, binding

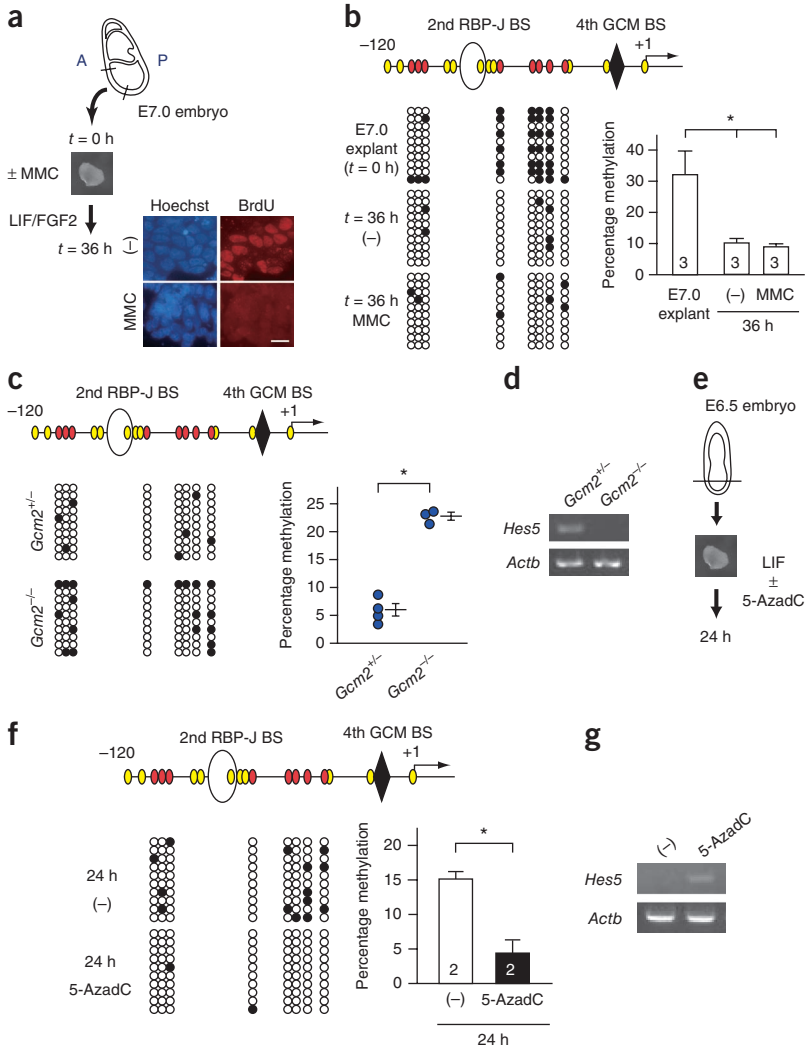

Figure 7 Active demethylation by Gcms *in vivo*. (**a**) A scheme of explant culture from E7.0 embryos. Head primordium was incubated with mitomycin C (MMC) for 2 h and then cultured in the presence of LIF and FGF2. The explants were immunostained for BrdU that had been added to the culture 2 h before fixation. Scale bar, 20 μm. (**b**,**c**,**f**) Methylation status of the *Hes5* promoter in explants from E7.0 or E6.5 embryos. Left, methylation status of the *Hes5* promoter analyzed by bisulfite sequencing. Closed and open circles indicate methylated and nonmethylated CpG sites, respectively. Right, methylation frequency of CpG sites in the *Hes5* proximal promoter region. (**b**) Methylation analysis of explants from E7.0 embryos and MMC-treated explants cultured for 36 h. (**c**,**d**) Head primordium of E7.0 *Gcm2* mutant embryos was incubated with MMC for 2 h and then cultured in the presence of LIF and FGF2. After 36 h in culture, the explants were subjected to bisulfite sequencing (**c**) and RT-PCR (**d**). (**e**) Scheme of explant culture from E6.5 embryos. The distal portion of E6.5 embryos was excised and cultured in serum-free medium containing LIF, in the presence or absence of 1 μM 5-AzadC. (**f**,**g**) After 24 h in culture, the explants were subjected to bisulfite sequencing (**f**) and RT-PCR (**g**). Error bars, s.e.m.; *n* values shown in columns. $^*P < 0.05$ by one-way ANOVA followed by Dunnett's *post hoc* comparison (**b**) or by Student's *t* test (**c**,**f**).

of Gcm1 or Gcm2 to chromatin containing the fourth as well as the second GCM binding site was verified by ChIP analysis in Neuro2a cells overexpressing FLAG-tagged *Gcms* (**Supplementary Fig. 7a–c**). Gcm2, but not Gcm1, bound to chromatin containing the fourth GCM binding site in STO cells, in which the *Hes5* promoter is highly methylated (**Supplementary Fig. 7d**).

Evidence for replication-independent active DNA demethylation is accumulating in mammals[23,25–28]. A possible mechanistic explanation for active DNA demethylation involves deamination of 5-methylcytosine to thymine, coupled with G/T mismatch repair[22]. Recently, 5-methyl-CpG binding domain protein 4 (MBD4), which recognizes methyl CpG and possesses thymidine glycosylase activity, has been reported to be involved in this process[27,29]. After the removal of thymidine at G/T mismatch base pairs by MBD4, cytosine is reinstalled through an excision-repair mechanism. All of the genes that are involved in this model were expressed in the head primordium of E7.5 embryos and some of them were downregulated by E8.5 (**Supplementary Fig. 8a**). Although all of those genes were expressed in STO cells and mouse embryonic fibroblasts (MEFs), the expression of the genes responsible for the deamination of 5-methylcytosine, *Aicda* (activation-induced cytidine deamidase, AID) and *Apobec1*, could not be detected in Neuro2a cells. To test whether MBD4 is involved in the demethylation of the *Hes5* promoter by Gcms, we transfected methylated and naive reporter plasmids into MEFs derived from wild-type and *Mbd4*$^{-/-}$ mouse embryos. NICD restored promoter activity in both wild-type and *Mbd4*$^{-/-}$ MEFs when both *Gcm1* and *Gcm2* expression plasmids were co-transfected ($F_{(3,8)} = 68.78$, $P < 0.0001$ for wild-type; $F_{(3,8)} = 93.11$, $P < 0.0001$ for *Mbd4*$^{-/-}$; **Supplementary Fig. 8b**). Consistent with these findings, the expression of *Hes5* was preserved in *Mbd4*$^{-/-}$ embryos at E9.5 (**Supplementary Fig. 8c**). These results suggest that *Gcm1* and *Gcm2* are important for the demethylation of the *Hes5* promoter, which is a chromosome replication-independent (active) process, but that the proposed mechanism of active demethylation does not occur in this process.

Gcms are responsible for active demethylation in early embryos

To test whether the demethylation of the *Hes5* promoter in E7.5–9.5 embryos was an active process, we used explant cultures of head primordium from E7.0 embryos (**Fig. 7a**). The methylation of the *Hes5* promoter in the explants decreased after 36 h in culture, which corresponds to E8.5 (**Fig. 7b**). Some explants were first mitotically inactivated by incubating with mitomycin C, and inactivation was verified by the absence of BrdU incorporation (**Fig. 7a**). The methylation frequency of the *Hes5* promoter in the mitomycin C-treated explants was comparable to that in the naive explants, which was significantly lower than in the explants before the culture ($F_{(2,6)} = 8.423$, $P = 0.0181$; **Fig. 7b**), suggesting that this demethylation is independent of replication. We next examined whether this demethylation in the explant culture was impaired in the absence of *Gcm2*, because the methylation of the *Hes5* promoter was significantly higher in E8.33 *Gcm2*$^{-/-}$ embryos than in littermate controls (**Fig. 2d**). Explants of

head primordium from E7.0 *Gcm2* mutants that had been treated with mitomycin C were analyzed for methylation status after 36 h in culture. The methylation frequency in the explants from E7.0 $Gcm2^{-/-}$ embryos was significantly higher than that from $Gcm2^{+/-}$ and $Gcm2^{+/+}$ controls ($t_{(5)} = 11.63$, $P < 0.0001$; **Fig. 7c**). We then tested whether *Hes5* was induced in the mitomycin C–treated explants from E7.0 embryos and found that, consistent with the demethylation of the promoter, *Hes5* mRNA could be detected by RT-PCR (**Fig. 7d**). By contrast, as a result of impaired demethylation of the promoter, *Hes5* mRNA was absent in the mitomycin C–treated explants from E7.0 $Gcm2^{-/-}$ embryos, as confirmed by quantitative RT-PCR ($1.605 \pm 0.121 \times 10^{-3}$ (mean ± s.e.m.) for *Hes5*/*Actb* in $Gcm2^{+/+}$ and $Gcm2^{+/-}$ ($n = 3$), $0.228 \pm 0.114 \times 10^{-3}$ for *Hes5*/*Actb* in $Gcm2^{-/-}$ ($n = 2$), $t_{(3)} = 7.754$, $P = 0.0045$; **Fig. 7d**). Thus, the demethylation of the *Hes5* promoter in the mouse head primordium during E7.5–9.5 is a chromosome replication–independent, *Gcm2*-dependent process.

Finally, we determined whether demethylation of the promoter was sufficient to induce *Hes5* in explant cultures from E6.5 embryos. The distal portion of E6.5 embryos, the visceral endoderm of which is rotated to the anterior portion and induces the head primordium in later development[30], was cultured in the presence of a DNA methyltransferase inhibitor, 5-aza-2′-deoxycytidine (5-AzadC) for 24 h (**Fig. 7e**). Incubation with 5-AzadC resulted in significantly lower methylation of the *Hes5* promoter in the explants than in untreated explants after 24 h in culture, which corresponds to E7.5, safely before the induction of *Hes5 in vivo* ($t_{(2)} = 4.965$, $P = 0.0383$; **Fig. 7f**). After the demethylation, *Hes5* expression was induced in the 5-AzadC–treated but not in the untreated explants, as confirmed by quantitative RT-PCR ($0.608 \pm 0.112 \times 10^{-3}$ for *Hes5*/*Actb* in control ($n = 4$), $2.891 \pm 0.925 \times 10^{-3}$ for *Hes5*/*Actb* in 5-AzadC–treated explants ($n = 4$), $t_{(6)} = 2.450$, $P = 0.0498$; **Fig. 7g**).

DISCUSSION

DNA methylation and demethylation is one of the epigenetic mechanisms that determine strictly regulated gene expression, and active DNA demethylation is pivotal in many developmental and physiological processes[22,23,25–29]. However, the existence of 5-methylcytosine demethylase has been doubted because cleavage of 5-methylcytosine to cytosine and methanol requires high activation energy, and is therefore unlikely to occur[21]. Instead, another model that consists of deamination of 5-methylcytosine to thymine and excision-repair of the G/T mismatch was recently proposed[22]. MBD4 can participate in the latter process because MBD4 is the only member of the 5-methyl-CpG binding domain proteins that possesses G/T mismatch repair DNA glycosylase activity[27,29]. The demethylation of the *Hes5* promoter by Gcm proteins shown here is a DNA replication–independent active process but occurs in the absence of MBD4. It is possible that another G/T mismatch repair DNA glycosylase, TDG, is responsible for it[31]. However, we think this process has only a minor role, if any, because methylated plasmids were demethylated after the overexpression of *Gcm1* and *Gcm2* in mitotically inactive Neuro2a cells, which barely express *Aicda* or *Apobec1*, the genes that are responsible for the deamination of 5-methylcytosine. It is still possible that, in the 5-methylcytosine deamination–G/T mismatch repair model, Gcms can substitute for Aicda and Apobec1 or MBD4 and TDG, or both. Alternatively, Gcms might induce the demethylation of the *Hes5* promoter by mechanisms other than 5-methylcytosine deamination coupled with G/T mismatch repair, although there is no evidence for these mechanisms in mammals[22]. Although molecules that are involved in the 5-methylcytosine deamination–G/T mismatch repair model are ubiquitously expressed, active demethylation occurs in specific DNA regions in a temporally and spatially regulated fashion. Gcms may provide a signal for the timing and location of demethylation because deletion of the GCM binding site near to methylated CpG sites in the *Hes5* promoter repressed demethylation.

Gcm1 and Gcm2 contain no known domain structures and show little homology with each other on the primary amino acid sequences except for the DNA-binding GCM domain[12,13]. Nevertheless, they are, at least in part, functionally redundant because reduction of *Hes5* expression was much more severe in E8.33 $Gcm1^{-/-}; Gcm2^{-/-}$ embryos than in $Gcm2^{-/-}$ embryos. Our data suggest that Gcm2 is important for demethylation through binding to the fourth GCM binding site in the proximal promoter and that Gcm1 and 2 cooperatively transactivate *Hes5* expression by binding to the distal promoter containing the second GCM binding site in cells that are in a low methylation state in the *Hes5* promoter. It is possible that Gcm2 modifies the expression of other unidentified genes by demethylating promoter regions because $Gcm2^{-/-}$ embryos show severe defects in the CNS until E10.5. This is despite the finding that null mutants for *Hes5* alone show few phenotypes in the brain[32], possibly due to the redundancy of function shared by *Hes* family genes[33]. One of the phenotypes of $Gcm2^{-/-}$ mutants, opening of the anterior neuropore, has been reported in E9.5 $Rbpj^{-/-}$ embryos[34], which present the severest phenotypes among null mutants for Notch pathway genes. Taking into account the findings that Gcms regulate the access of RBP-J to the *Hes5* promoter by demethylation, Gcms could modify the RBP-J-mediated expression of genes other than *Hes5*. It is necessary to investigate the biochemical characteristics of Gcms and to identify molecule(s) or gene(s) with which Gcms interact.

The Notch receptor-mediated lateral inhibition model has been widely accepted as a theoretical basis to explain the sustained Notch signaling activation that is seen in neural stem cells that receive ligand stimuli from differentiating progeny cells in the developing brain[35]. This model is also considered to explain the 'salt-and-pepper pattern' of *Hes1* and *Dll1* expression in the early nervous system[36,37]. However, recent observations that Hes1 levels oscillate in neural precursors, and that Hes1 oscillation in turn induces the inverse oscillation of *Dll1* and a proneural gene *Neurogenin2,* have challenged the validity of the lateral inhibition model[35,38,39]. Ligand-expressing and ligand-receiving neural precursor cells could alter, in a short amount of time, their roles with respect to each other, and therefore, *Hes1* expression in the E7.5–8.5 neuroepithelium would not predict that those cells will become neural stem cells in later brains[35]. By contrast, *Hes5* mRNA is only detectable at E8.33 and afterwards[2], and *Hes5* seems to be continuously expressed because the oscillation of Hes5 levels in forebrain neural precursors has not been shown. Therefore, *Hes5* expression induced by *Gcm* genes around E8.33 first by the demethylation of its promoter and then by transactivation (**Supplementary Fig. 9**) could act as a selection signal for the fate of neural stem cells by continuously suppressing the expression of Notch ligand and proneural genes. After neural differentiation starts at E9.5 in the forebrain, the *Hes5*-expressing cells could receive ligand stimuli from differentiating neural progenitor cells that express *Dll1,* and activate the canonical Notch signaling (**Supplementary Fig. 9**). Thus, those cells are later maintained as neural stem cells in the developing forebrain.

METHODS

Methods and any associated references are available in the online version of the paper at http://www.nature.com/natureneuroscience/.

Note: Supplementary information is available on the Nature Neuroscience website.

ACKNOWLEDGMENTS

We thank R. Kageyama, J.S. Nye, T. Miyazaki and T. Honjo for plasmids, T.-e.U and Y. Imai for MBD4 mutant mice, and R. Kageyama, D. van der Kooy and K. Nakashima for comments. This work was supported by a Grant-in-Aid for Exploratory Research (19650096) from the Ministry of Education, Culture, Sports, Science and Technology of Japan (K.I.S.H.).

AUTHOR CONTRIBUTIONS

S.H. designed and carried out the experiments, analyzed the data and wrote the paper. Y.I., A.K., S.J., K.F.T. and T.H. generated *Gcm* mutant mice and analyzed the phenotypes. T.K. and S.K. carried out the experiments related to MBD4 knockout mice. Y.H. and K.I. supervised the project.

COMPETING FINANCIAL INTERESTS

The authors declare no competing financial interests.

Published online at http://www.nature.com/natureneuroscience/.
Reprints and permissions information is available online at http://www.nature.com/reprints/index.html.

1. Reynolds, B.A., Tetzlaff, W. & Weiss, S. A multipotent EGF-responsive striatal embryonic progenitor cell produces neurons and astrocytes. *J. Neurosci.* **12**, 4565–4574 (1992).
2. Hitoshi, S. *et al.* Primitive neural stem cells from the mammalian epiblast differentiate to definitive neural stem cells under the control of Notch signaling. *Genes Dev.* **18**, 1806–1811 (2004).
3. Nakamura, Y. *et al.* The bHLH gene *Hes1* as a repressor of the neuronal commitment of CNS stem cells. *J. Neurosci.* **20**, 283–293 (2000).
4. Ohtsuka, T., Sakamoto, M., Guillemot, F. & Kageyama, R. Roles of the basic helix-loop-helix genes Hes1 and Hes5 in expansion of neural stem cells of the developing brain. *J. Biol. Chem.* **276**, 30467–30474 (2001).
5. Hitoshi, S. *et al.* Notch pathway molecules are essential for the maintenance, but not the generation, of mammalian neural stem cells. *Genes Dev.* **16**, 846–858 (2002).
6. Artavanis-Tsakonas, S., Rand, M.D. & Lake, R.J. Notch signaling: cell fate control and signal integration in development. *Science* **284**, 770–776 (1999).
7. de la Pompa, J.L. *et al.* Conservation of the Notch signalling pathway in mammalian neurogenesis. *Development* **124**, 1139–1148 (1997).
8. Donoviel, D.B. *et al.* Mice lacking both presenilin genes exhibit early embryonic patterning defects. *Genes Dev.* **13**, 2801–2810 (1999).
9. Hosoya, T., Takizawa, K., Nitta, K. & Hotta, Y. *glial cells missing*: a binary switch between neuronal and glial determination in *Drosophila*. *Cell* **82**, 1025–1036 (1995).
10. Jones, B.W., Fetter, R.D., Tear, G. & Goodman, C.S. *glial cells missing*: a genetic switch that controls glial versus neuronal fate. *Cell* **82**, 1013–1023 (1995).
11. Jones, B.W. Transcriptional control of glial cell development in *Drosophila*. *Dev. Biol.* **278**, 265–273 (2005).
12. Akiyama, Y., Hosoya, T., Poole, A.M. & Hotta, Y. The gcm-motif: a novel DNA-binding motif conserved in *Drosophila* and mammals. *Proc. Natl. Acad. Sci. USA* **93**, 14912–14916 (1996).
13. Schreiber, J., Sock, E. & Wegner, M. The regulator of early gliogenesis *glial cells missing* is a transcription factor with a novel type of DNA-binding domain. *Proc. Natl. Acad. Sci. USA* **94**, 4739–4744 (1997).
14. Egger, B. *et al.* Gliogenesis in *Drosophila*: genome-wide analysis of downstream genes of *glial cells missing* in the embryonic nervous system. *Development* **129**, 3295–3309 (2002).
15. Kim, J. *et al.* Isolation and characterization of mammalian homologs of the *Drosophila* gene *glial cells missing*. *Proc. Natl. Acad. Sci. USA* **95**, 12364–12369 (1998).
16. Günther, T. *et al.* Genetic ablation of parathyroid glands reveals another source of parathyroid hormone. *Nature* **406**, 199–203 (2000).
17. Schreiber, J., Enderich, J. & Wegner, M. Structural requirement for DNA binding of GCM proteins. *Nucleic Acids Res.* **26**, 2337–2343 (1998).
18. Schreiber, J. *et al.* Placental failure in mice lacking the mammalian homolog of glial cells missing, GCMa. *Mol. Cell. Biol.* **20**, 2466–2474 (2000).
19. Hatakeyama, J. *et al.* Hes genes regulate size, shape and histogenesis of the nervous system by control of the timing of neural stem cell differentiation. *Development* **131**, 5539–5550 (2004).
20. Martens, D.J., Tropepe, V. & van der Kooy, D. Separate proliferation kinetics of fibroblast growth factor–responsive and epidermal growth factor–responsive neural stem cells within the embryonic forebrain germinal zone. *J. Neurosci.* **20**, 1085–1095 (2000).
21. Wolffe, A.P., Jones, P.L. & Wade, P.A. DNA demethylation. *Proc. Natl. Acad. Sci. USA* **96**, 5894–5896 (1999).
22. Zhu, J.-K. Active DNA demethylation mediated by DNA glycosylases. *Annu. Rev. Genet.* **43**, 143–166 (2009).
23. Reik, W. Stability and flexibility of epigenetic gene regulation in mammalian development. *Nature* **447**, 425–432 (2007).
24. Waga, S. & Stillman, B. The DNA replication fork in eukaryotic cells. *Annu. Rev. Biochem.* **67**, 721–751 (1998).
25. Bruniquel, D. & Schwartz, R.H. Selective, stable demethylation of the interleukin-2 gene enhances transcription by an active process. *Nat. Immunol.* **4**, 235–240 (2003).
26. Ma, D.K. *et al.* Neuronal activity-induced Gadd45b promotes epigenetic DNA demethylation and adult neurogenesis. *Science* **323**, 1074–1077 (2009).
27. Kim, M.-S. *et al.* DNA demethylation in hormone-induced transcriptional derepression. *Nature* **461**, 1007–1012 (2009).
28. Okada, Y., Yamagata, K., Hong, K., Wakayama, T. & Zhang, Y. A role for the elongator complex in zygotic paternal genome demethylation. *Nature* **463**, 554–558 (2010).
29. Rai, K. *et al.* DNA demethylation in zebrafish involves the coupling of a deaminase, a glycosylase, and Gadd45. *Cell* **135**, 1201–1212 (2008).
30. Kimura, C. *et al.* Visceral endoderm mediates forebrain development by suppressing posteriorizing signals. *Dev. Biol.* **225**, 304–321 (2000).
31. Zhu, B. *et al.* 5-Methylcytosine-DNA glycosylase activity is present in a cloned G/T mismatch DNA glycosylase associated with the chicken embryo DNA demethylation complex. *Proc. Natl. Acad. Sci. USA* **97**, 5135–5139 (2000).
32. Cau, E., Gradwohl, G., Casarosa, S., Kageyama, R. & Guillemot, F. *Hes* genes regulates sequential stages of neurogenesis in the olfactory epithelium. *Development* **127**, 2323–2332 (2000).
33. Kageyama, R., Ohtsuka, T. & Kobayashi, T. The Hes gene family: repressors and oscillators that orchestrate embryogenesis. *Development* **134**, 1243–1251 (2007).
34. Oka, C. *et al.* Disruption of the mouse *RBP-Jκ* gene results in early embryonic death. *Development* **121**, 3291–3301 (1995).
35. Kageyama, R., Ohtsuka, T., Shimojo, H. & Imayoshi, I. Dynamic Notch signaling in neural progenitor cells and a revised view of lateral inhibition. *Nat. Neurosci.* **11**, 1247–1251 (2008).
36. Bettenhausen, B., Hrabě de Angelis, M., Simon, D., Guénet, J.L. & Gossler, A. Transient and restricted expression during mouse embryogenesis of Dll1, a murine gene closely related to *Drosophila* Delta. *Development* **121**, 2407–2418 (1995).
37. Hatakeyama, J. & Kageyama, R. Notch1 expression is spatiotemporally correlated with neurogenesis and negatively regulated by Notch1-independent Hes genes in the developing nervous system. *Cereb. Cortex* **16** (suppl. 1), i132–i137 (2006).
38. Hirata, H. *et al.* Oscillatory expression of the bHLH factor Hes1 regulated by a negative feedback loop. *Science* **298**, 840–843 (2002).
39. Shimojo, H., Ohtsuka, T. & Kageyama, R. Oscillations in Notch signaling regulate maintenance of neural progenitors. *Neuron* **58**, 52–64 (2008).

ONLINE METHODS

Disruption of *Gcm1* and *Gcm2* genes. To construct a targeting vector for *Gcm1*, a 4.3-kb genomic fragment containing the 5′ non-coding exon and the translational start site as a 5′ recombination arm, and a 3.8-kb *Bam*HI genomic fragment containing the sixth exon as a 3′ recombinant arm were subcloned into the IRES-βgal-LoxPNeoSVpA vector. To construct a targeting vector for *Gcm2*, a 4.2-kb *Xba*I-*Apa*I genomic fragment containing the translational start site as a 5′ recombination arm, and a 4.7-kb *Hin*dIII genomic fragment containing the fifth exon as a 3′ recombinant arm were subcloned into the same vector. The targeting vectors were electroporated into embryonic stem cells (129SVJ/RW-4), and G418-resistant embryonic stem cell clones were injected into blastocysts, and implanted into pseudopregnant mice. The resulting chimeric mice were bred with C57/BL6 mice to generate mice heterozygous for the targeted allele. Unfortunately, due to a frame-shift mutation that had been introduced to the *lacZ* gene used to construct the targeting vectors, we were unable to detect *Gcm1*- or *Gcm2*-expressing cells by X-gal staining.

Mice and genotyping. Mice heterozygous for *Gcm1* and/or *Gcm2* were maintained either in the CD1 or C57/BL6 background. Genotyping of *Mbd4* (Jackson Laboratory) mutant mice maintained in the C57/BL6 background was as described[27]. PCR analysis was used for routine genotyping using the following primers; gcm1-F1 (5′-CACGGCAATCGGCAATCT-3′), gcm1-R1 (5′-AGCTCTAAAGGCGTTCAC-3′), gcm1-R2 (5′-AGGTGTGCACTGCTATGC-3′), gcm2-F1 (5′-GCACGCCAAGGGTGCATTTA-3′), gcm2-R1 (5′-AGGTCTTGCCAGTCAGTC-3′) and cassette-F1 (5′-CATAGCCTGAAGAACGAG-3′) for *Gcm1* and *Gcm2* alleles as described. Midday of the plugged day was set as E0.5. All experiments were carried out with permission of the institutional Animal Research Committee of the National Institute of Physiological Sciences.

Molecular biology. Full-length *Gcm1* and *Gcm2* genes were amplified by RT-PCR from E12.5 placental cDNA, sequenced and subcloned into the pCX expression vector (a gift from T. Miyazaki, Osaka University) to generate Gcm1-pCX and Gcm2-pCX, respectively. Full-length *Hes5* (a gift from R. Kageyama, Kyoto University) and a construct encoding an active form of Notch1, NICD (a gift from J.S. Nye, Northwestern University), were subcloned into pCX. Constructs encoding type and dominant negative forms of RBP-J in a pCMX-N expression vector were provided by RIKEN BRC DNA Bank. *Mbd4* in a pcDNA3.1 expression vector was as described[27].

RT-PCR. Total RNA isolation, cDNA synthesis and RT-PCR analysis were carried out as described[5]. cDNA was amplified in a thermal cycler with denaturation at 95 °C for 30 s, annealing at 56 °C for 40 s and extension at 72 °C for 40 s for 30 (*Actb*), 35 (*Gadd45a, Gadd45b*, *Aicda*, *Apobec1* and *Tdg*) or 40 cycles (*Hes5*, *Gcm1*, *Rbpj* and *Mbd4*). The sense and antisense primers used were as follows: hes5-F1 (5′-AAGTACCGTGGCGGTGGAGATGC-3′), hes5-R1 (5′-CGCTGGAAGTGGTAAAGCAGCTT-3′), gcm1-F2 (5′-GACAACTCGAGTAGAGAAGAGCC-3′), gcm1-R3 (5′-GGAGGCAGATGCCATGTGCAC-3′), rbp-j-F1 (5′-TGGCACTGTTCAATCGCCTT-3′), rbp-j-R1 (5′-AATCTTGGGAGTGCCATGCCA-3′), gadd45a-sense (5′-GCACTTGCAATATGACTTTG-3′), gadd45a-antisense (5′-CGGATGCCATCACCGTTCCG-3′), gadd45b-sense (5′-GTGACTGCATCATGACCCTG-3′), gadd45b-antisense (5′-TTGGAGTGGGTCTCAGCGTT-3′), Aicda-sense (5′-GACCGATATGGACAGCCTTC-3′), Aicda-antisense (5′-AGGTTGCTTTCAAAATCCCA-3′), apobec1-sense (5′-CAGAGCAAGATGAGTTCCGA-3′), apobec1-antisense (5′-ACTCCCAGAAGTCATTTCAA-3′), MBD4-sense (5′-AAAGCAGCAGGGATGGAGAG-3′), MBD4-antisense (5′-CCTTTCGGCAGTACAGTAAA-3′), TDG-sense (5′-ACTTGGAATTTGGGCTTCAA-3′), TDG-antisense (5′-CTGAGAGGCACCCTTCCTAA-3′), actb-F1 (5′-AGGCCAACCGTGAAAAGATGAC-3′), and actb-R1 (5′-GTACATGGTGGTACCACCAGAC-3′). Nested PCR was used to determine the expression of *Gcm2*. The first amplification was performed using the gcm2-F1 and gcm2-R2 (5′-CATTCCAACTCTCAACAGCA-3′) primers with the same reaction conditions as above for 30 cycles. The resulting reaction mixture was diluted tenfold and used for the second PCR using the gcm2-F2 (5′-GCAATATCCTGGTTTGAC-3′) and gcm2-R1 primers.

Luciferase reporter assay. The promoter regions of the *Hes5*, *Gcm1* or *Gcm2* genes were ligated to firefly luciferase reporter plasmids (TOYO B-Net). The *Hes5* promoters with various lengths of deletions or with mutations at the second (TGAGGGT -> TCGACGT) or fourth (TGCTGGG -> TGCTGCA) GCM binding sites were also used. Cells were transfected with a luciferase reporter plasmid together with a synthetic *Renilla* luciferase reporter plasmid (Promega) as an internal control, using FuGENE6 (Roche). Luciferase activities were determined by a Dual-Luciferase Reporter Assay System (Promega).

Chromatin immunoprecipitation assay. Chromatin samples prepared from Neuro2a or STO cells were subjected to immunoprecipitation with an anti-RBP-J antibody (Santa Cruz Biotechnology) by means of LowCell# ChIP Kit (Diagenode) according to the manufacturer's protocol. Chromatin samples prepared from Neuro2a or STO cells overexpressing FLAG-tagged genes were subjected to immunoprecipitation with an anti-FLAG antibody (M2; Sigma). DNA was PCR amplified with denaturation at 95 °C for 30 s, annealing at 60 °C for 30 s and extension at 72 °C for 30 s for 30 cycles using hes5-F2 (5′-CCTCTGGGGAGTGGGAGGGAA-3′) and hes5-R2 (5′-GCCATGCCTGGAGCTCTGGAG-3′) primers. PCR amplification using hes5-F4 (5′-CAAGAGCCTGCACCAGGACTA-3′) and hes5-R4 (5′-CGGTCGGCCGCTGGGTCACCA-3′) primers was used for negative controls. Chromatin samples were also prepared from E8.5 wild-type or *Gcm1* mutant embryos and were subjected to immunoprecipitation with an anti-GCM1 antibody (AVIVA Systems Biology). Extracted DNA was PCR amplified using the hes5-F3 (5′-AACCACCAGACTCCTCTTCCTT-3′) and hes5-R3 (5′-AGGCAGCACAGGATGGTCTGT-3′) primers or using hes5-F4 and hes5-R4 primers.

Bisulfite sequencing and plasmid methylation. Genomic DNA was isolated from Neuro2a cells and STO cells, which were transfected with the empty pCX expression vector, Gcm1-pCX, Gcm2-pCX, or Gcm1-pCX and Gcm2-pCX together. Genomic DNA was also extracted from E7.5 anterior neuroectoderm and visceral endoderm (head primordium), E8.5 forebrain and midbrain, or E9.5 forebrain of wild-type mice, or from forebrain and midbrain of E8.33 *Gcm1* and *Gcm2* mutants. Bisulfite reactions were performed using an EpiTect Bisulfite Kit (Qiagen) according to the manufacturer's protocol, and specific DNA fragments containing RBP-J binding sites in the *Hes5* promoter were amplified by PCR using hes5-F5m (5′- GGAGAGAAGGGGGGGGAGA -3′) and hes5-R5m (5′-AACACACCAACCCTATATAAAC -3′) primers. The PCR products were cloned into p123T vector (Mo Bi Tec, Germany) and 10 clones randomly chosen from three independent PCR amplifications were sequenced.

Firefly luciferase reporter plasmid containing the *Hes5* promoter region from base pairs −692 to +73 was treated with the HhaI methylase, which converts the first cytosine of the GCGC sequence to a 5-methylcytosine. More than 90% efficiency of methylation was verified by digesting the resultant plasmid with a methylation-sensitive restriction enzyme *Nar*I that recognizes GGCGCC. The methylated plasmid was transfected into nonmurine COS1 cells together with empty pCX or both Gcm1-pCX and Gcm2-pCX. Three days after transfection the cells were washed and treated with DNase I to remove any untransfected plasmid in the medium. The transfected plasmids were then recovered from the cells and subjected to bisulfite sequencing.

***In utero* electroporation.** *In utero* electroporation was performed as described[40]. Three micrograms of plasmid consisting of Gcm1-pCX (2.8 μg), Gcm2-pCX (2.8 μg), Gcm1-pCX and Gcm2-pCX (1.4 μg each), Hes5-pCX (2.8 μg) or pCX (2.8 μg) together with GFP-pCX (0.2 μg) in 1 μl was injected into the lateral ventricles of E14.5 CD1 mouse embryos through the uterus. After injection, each embryo in the uterus was placed between the electrodes (CUY650P3, CUY661-3X7 with CUY661N, NEPA GENE) and given five 50-ms pulses of 33 V, with 950-ms intervals, by an electroporator (CUY21, NEPA GENE). The uterus was placed back into the abdominal cavity for continued embryonic development for 24 h. BrdU (50 mg kg^{-1}) was intraperitoneally administered to the dam 2 h before perfusion with 4% paraformaldehyde. Brains were removed from the embryos, post-fixed with the same fixative overnight, and cryoprotected with 20% sucrose in PBS at 4 °C.

Coronal cryosections at a thickness of 14 μm were subjected to immunostaining. We used anti-GFP (rat monoclonal IgG; 1:2,000; Nacalai Tesque), anti-Pax6 (rabbit polyclonal IgG; 1:1,000; Millipore), anti-Tbr2 (rabbit polyclonal IgG; 1:1,000; Millipore), anti-BrdU (mouse monoclonal IgG; 1:3,000; BD Biosciences), anti-nestin (rabbit polyclonal IgG; 1:1,000; IBL) and anti-βIII tubulin (mouse

monoclonal IgG; 1:3,000; Sigma) antibodies as primary antibodies, followed by appropriate Alexa-conjugated goat secondary antibodies (Molecular Probes). For the detection of GFP and BrdU, sections were incubated with the anti-GFP antibody at 4 °C overnight, followed by the Alexa488-conjugated goat secondary antibody. Then, the sections were boiled in citrate buffer (pH 6.0) for 7 min and treated with the anti-BrdU antibody at 4 °C overnight, followed by the Alexa568-conjugated goat secondary antibody. Sections were finally counter-labeled with the nuclear stain Hoechst 33342 (1 μg ml^{-1}; Sigma).

***In situ* hybridization and whole mount *in situ* hybridization.** Digoxigenin (DIG)-labeled single strand riboprobes for the *Gcm1*, *Gcm2*, *Hes1*, *Hes3*, *Hes5*, *Ngn2* or *Mash1* genes were synthesized using the entire coding region of the cDNAs for each gene as a template in a DIG RNA labeling mix (Roche). *In situ* hybridization using cryosections was performed as described[41]. For whole mount *in situ* hybridization, mouse embryos at E8.33–9.5 were fixed in 4% paraformaldehyde for 6 h, dehydrated in serial concentrations of ethanol and stored in 80% ethanol at −20 °C. Samples were rehydrated, treated with 10 μg ml^{-1} proteinase K for 4–8 min and post-fixed in 4% paraformaldehyde for 1 h. Hybridization was performed for 16 h at 65 °C in 50% formamide, 5× SSC, 1× Denhardt's solution, 0.2 mg ml^{-1} yeast tRNA, 0.1 mg ml^{-1} heparin, 5 mM EDTA, 0.1% Tween 20, 0.1% CHAPS and 300 ng ml^{-1} probe. The samples were washed and then treated with 10 μg ml^{-1} RNase A for 30 min in 10 mM Tris, pH 7.5, 0.5 M NaCl and 0.1% Tween 20 to remove any unhybridized probe. The samples were extensively washed, and hybridized DIG-labeled RNA probes were visualized with alkaline phosphatase-conjugated anti-DIG antibody (1:2,000; Roche) and an nitro-blue tetrazolium/5-bromo-4-chloro-3′-Indolylphosphatase reaction.

***In vitro* induction of neural stem cells and neurosphere assay.** Cell culture from E7.5 mouse embryos was carried out as described[2] with slight modifications. Briefly, prospective head regions from E7.5 mouse embryos at late primitive streak stage or at early headfold stage were excised and cultured in serum-free medium containing 1×10^3 U ml^{-1} LIF (Chemicon). After 5 d, the primary explant was mechanically triturated into single cells by pipetting. The cells were cultured in serum-free medium in the presence of both LIF and 10 ng ml^{-1} FGF2, together with 2 μg ml^{-1} of heparin for 7 d. The resulting secondary spheres were again collected, triturated and cultured in serum-free medium containing 10 ng ml^{-1} FGF2 and 20 ng ml^{-1} EGF. Extraembryonic tissue from each embryo was subjected to genotyping.

The protocol used to generate neurospheres *in vitro* from embryonic brains has been described[5]. Briefly, neural tissue was excised from the forebrain of E9.5 mouse embryos and cells were triturated in serum-free medium and cultured in the presence of 10 ng ml^{-1} FGF-2 together with 2 μg ml^{-1} heparin. After 6 days *in vitro*, the numbers of floating sphere colonies (neurospheres) with diameter >0.08 mm were counted.

Explant culture of early embryos. Prospective head regions from E7.0 mouse embryos at late primitive streak stage were excised and cultured in serum-free medium containing 1×10^3 U ml^{-1} LIF and 10 ng ml^{-1} FGF2, together with 2 μg ml^{-1} of heparin. The explants were first incubated with 10 μg ml^{-1} of mitomycin C for 2 h, washed, and then cultured in the same medium. In some of the culture, 10 μM of BrdU was added 2 h before fixation by 4% paraformaldehyde. From other explants, genomic DNA was extracted and subjected to bisulfite sequencing analysis.

The distal portion of E6.5 embryos was excised and cultured in serum-free medium containing 1×10^3 U ml^{-1} LIF, in the presence or absence of the DNA methyltransferase inhibitor 5-AzadC at a concentration of 1 μM. After 24 h in culture, the explants were collected and subjected to bisulfite sequencing and RT-PCR analyses.

Statistics. Statistical analysis was performed using one-way ANOVA followed by Dunnett's *post hoc* comparison or using Kruskal-Wallis test followed by Dunn's test, or using an unpaired two-tailed Student's *t* test if applicable. Significance was set at $P < 0.05$.

40. Nakahira, E., Kagawa, T., Shimizu, T., Goulding, M.D. & Ikenaka, K. Direct evidence that ventral forebrain cells migrate to the cortex and contribute to the generation of cortical myelinating oligodendrocytes. *Dev. Biol.* **291**, 123–131 (2006).
41. Iwasaki, Y. *et al.* The potential to induce glial differentiation is conserved between *Drosophila* and mammalian glial cells missing genes. *Development* **130**, 6027–6035 (2003).

doi:10.1038/nn.2875